Controlled Preparation of Nitrogen-Doped Hierarchical Carbon Cryogels Derived from Phenolic-Based Resin and Their CO_2 Adsorption Properties

Yalan Zhou[1], Lu Luo[1], Wen Yan[1], Zeliang Li[1], Mizi Fan[3], Guanben Du[2], Weigang Zhao[*1]

[1]*College of Material Engineering, Fujian Agriculture and Forestry University, 63 Xiyuangong Road, Fuzhou 350002, PR China*

[2]*College of Material Science and Engineering, Southwest Forestry University, 300 Bailongsi, Kunming 650224, PR China*

[3]*College of Engineering, Design and Physical Sciences, Brunel University, Uxbridge UB8 3PH*

[*] Corresponding author
Tel: +86 180 5919 2996
e-mail: weigang-zhao@fafu.edu.cn

Abstract: Nitrogen-doped hierarchical carbon cryogels with good monolithic structure are synthesized from phenol (P), melamine (M), and formaldehyde (F) by sol-gel, freeze-drying, and carbonization process with different molar ratios of F/(P+M). The synthesized cryogels have the characteristics of cost-effective and abundant hierarchical pores. The pore structures, chemical properties, and CO_2 adsorption performance of the prepared carbon cryogels are investigated. The results reveal that the PF carbon cryogel without N doping shows poor porosity characteristics, which leads to lower CO_2 adsorption performance. For the N-doped PMF carbon cryogels, with the increase in the molar ratio of F/(P+M), the specific surface area and micropore volume decreases from 1160.6 to 874.1 m^2/g and from 0.47 to 0.35 cm^3/g, respectively, indicating that a lower formaldehyde content is conducive to the formation of more micropores and higher specific surface area. The carbon cryogel PMF2.0 (F/(P+M) = 2.0) exhibits a CO_2 adsorption capacity as high as 5.79 mmol/g, and it also has a high CO_2/N_2 adsorption selectivity (13.43) and isosteric adsorption heat (33.06 kJ/mol). Thus, the PMF carbon cryogel exhibits immense potential as an adsorbent for CO_2 capture, and its excellent performance is attributed to the synergistic effect of N doping and abundant micropores with appropriate size.

Keywords: Cryogel, Sol-gel process, Polycondensation, CO_2 adsorption, N-doped porous carbon, Hierarchical porosity

1 Introduction

The continuous increase in greenhouse effect due to human activities is causing rapid global warming, which has become a serious problem over the recent years. Therefore, the development of effective ways to reduce the impact of greenhouse gases on the environment has become a hot research topic. In particular, owing to its high concentration and long life, carbon dioxide, which is the main greenhouse gas, has received considerable attention [1, 2]. Presently, the materials used for CO_2 capture mainly include alcohol amine solution, porous solid materials, and separation membrane [3]. The porous solid materials, such as metal organic frameworks (MOFs) [4], activated carbons [5, 6], carbon gels [7, 8], carbon fibers [9], amine-functionalized fumed silica [10], zeolites [11], and porous polymers [12], are one of the most popular CO_2 capture materials due to their high adsorption capacity, easy regeneration, ease of operation, cost-effectiveness, durability, etc. [2, 3, 13].

Carbon gels are unique porous carbon materials with low bulk density, high electrical conductivity, hierarchical pore structure, and high specific surface area, which are widely used for energy storage [2, 14, 15], catalysis [16], supercapacitors [17, 18], adsorption [2, 19], and so on. It should be noted that the carbon gels also exhibit immense potential as a CO_2 capture material [1, 2]. Carbon gels can be prepared from various precursors, mainly by three steps: i) synthesis of hydrogel by sol-gel method; ii) solvent exchange and drying of hydrogels; iii) carbon aerogels are obtained by carbonization of organic aerogels [14, 15, 20]. The most traditional carbon gel materials are aerogels prepared from resorcinol and formaldehyde, and

their CO_2 adsorption properties have also been studied extensively [21, 22]. However, their raw material cost is quite high, and the commonly used supercritical drying process further increases the cost of the product, making their industrial production and applications quite challenging [3]. Therefore, significant efforts have been dedicated to improve the CO_2 adsorption performance and reduce the raw material and production costs. The first method is the partial or total substitution of resorcinol with some cheaper raw materials like phenol, urea, tannin, and lignin. The other way is to modify the synthesis methods, which can improve the product performance and further reduce the production costs.

During the preparation of carbon aerogels, the pore structure is mainly influenced by the molar ratio of raw materials, pH, dilution ratio, drying method, and carbonization conditions, which in turn affect the CO_2 adsorption performance significantly. Job et al. prepared resorcinol-formaldehyde carbon xerogels and found that the pH of the precursor solution could be adjusted to obtain the required pore structure [23, 24]. Li et al. used phenol to replace part of resorcinol for carbon cryogel preparation. It was found that the dilution ratio has a significant effect on the density, texture, structure, and CO_2 adsorption performance of carbon aerogel. The carbonization temperature, carbonization time, and heating rate of aerogel also affect the pore structure [25, 26]. Alain et al. found that carbon aerogels prepared by carbonization at 600 ℃ had the largest specific surface area, and a large number of micropores were generated below 1000 ℃ [25]. By changing the carbonization conditions, the pore structure could be controlled, thereby affecting the CO_2

adsorption capacity. Therefore, through reasonable adjustment of the synthesis process and conditions, a better functional design for CO_2 capture with reduced product cost can be obtained. Meanwhile, the cost of drying process is also a very important part of the total product cost. The existing drying methods for obtaining carbon gels mainly include supercritical drying, freeze drying, and atmospheric drying, which are used to prepare aerogel, cryogel, and xerogel, respectively [8]. The supercritical drying process is complex and expensive [27, 28]. On the other hand, atmospheric drying causes a serious volume shrinkage of the xerogel, resulting in quite high density and low porosity of aerogel [29, 30]. By comparison, freeze-drying method is more economical and convenient than traditional supercritical drying, and the volume shrinkage is not as serious as that in atmospheric drying [31, 32]. Therefore, freeze-drying is an effective and low-cost process to obtain cryogels with good pore structure.

The hydrophobicity of ordered porous carbon materials limits their adsorption capacity and CO_2 selectivity. The introduction of nitrogen can change the surface properties and acid-base properties as well as enhance the hydrophilicity of materials, thus it is an effective method to improve the CO_2 adsorption capacity and selectivity of porous carbon materials [7, 8, 21, 22]. In previous reports, nitrogen-containing materials, such as melamine [14, 15, 33], urea [7, 19], and ammonia [34], have been used as N source to synthesize various nitrogen-doped carbon gels, and these carbon gels achieved better performance due to the introduction of nitrogen. Muehlemann et al. found that the use of higher quality melamine resulted in the formation of a denser

aerogel with a greater hydrophilicity [20]. Kalijadis et al. used resorcinol and formaldehyde as raw materials and added different amounts of melamine to synthesize nitrogen-doped carbon cryogels, and they found that the introduction of nitrogen improved the catalytic and adsorption properties of carbon aerogels [33].

In this paper, cost-effective nitrogen-doped PMF carbon cryogels are prepared by sol-gel method using melamine (M) as the nitrogen source and low-cost phenol (P) and formaldehyde (F) as the main raw materials. These carbon cryogels with hierarchical structure are obtained by freeze-drying method as it is a simple, cheap, and convenient method. The effect of formaldehyde content (molar ratio of F/(P+M)) on the structure, morphology, and physicochemical properties of PMF carbon cryogel is examined. The CO_2 adsorption performance, including adsorption capacity, selective adsorption of CO_2/N_2, and heat of adsorption (Qst), is analyzed. Furthermore, the prepared PMF carbon cryogels are compared with PF carbon cryogel without N doping.

2 Experimental

2.1 Materials

Phenol (P, AR, >99.5%), melamine (M, AR, > 99.5%), formaldehyde (F, AR, 37% solution), sodium hydroxide (NaOH), and ethanol were purchased from the Shanghai Aladdin Biochemical Technology Co., Ltd.

2.2 Synthesis of carbon cryogel

The initial PMF resin was prepared as follows: a certain amount of phenol, melamine, formaldehyde, and magnetons were mixed in a flat bottom flask for

dissolution. The molar ratio of phenol to melamine (P/M) was fixed at 1/0.5, and the molar ratio of formaldehyde to phenol and melamine (F/(P+M)) was 2/1.5, 2.5/1.5, and 3/1.5. Then, 10 mol/L NaOH solution was used to adjust the pH of the mixed solution to 9.0. The temperature of the mixture was raised to 85 ℃ from room temperature, and it was kept in the condensation reflux state for 1 h to obtain initial transparent PMF resin.

The synthesized PMF resin was cooled to room temperature. Then, 10 g resin was mixed with aqueous ethanol solution as a diluent and sodium hydroxide solution as a catalyst. The pH of this mixture was adjusted to 9.0, and then it was transferred to an airtight glass tube and placed in an air blast drying oven under 100 °C for gelation and aging. After 5 days, the obtained hydrogel was removed from the glass container and placed in 15% aqueous ethanol solution for solvent exchange. The 15% ethanol aqueous solution was replaced with a fresh solution every day. This process was repeated 4 times to complete the solvent exchange process. The organic PMF cryogels were obtained by freezing the above gel in a freeze-dryer for 6 h and drying it at 20-50 Pa for 48 h. The organic cryogels were placed in a quartz boat and carbonized in a tubular furnace at a heating rate of 5 ℃/min and kept at 900 ℃ for 2 h. All the carbonization processes were conducted under continuous nitrogen protection at a flow rate of 80 mL/min, and the PMF carbon cryogels were finally obtained. For comparison, the PF cryogel without melamine was prepared with F/P molar ratio of 2/1.5. The samples of PMF carbon cryogels are labeled as PMF2.0, PMF2.5, PMF3.0, where the number after PMF represents the molar ratio of F/(P+M). The specific

preparation method is shown in Figure 1.

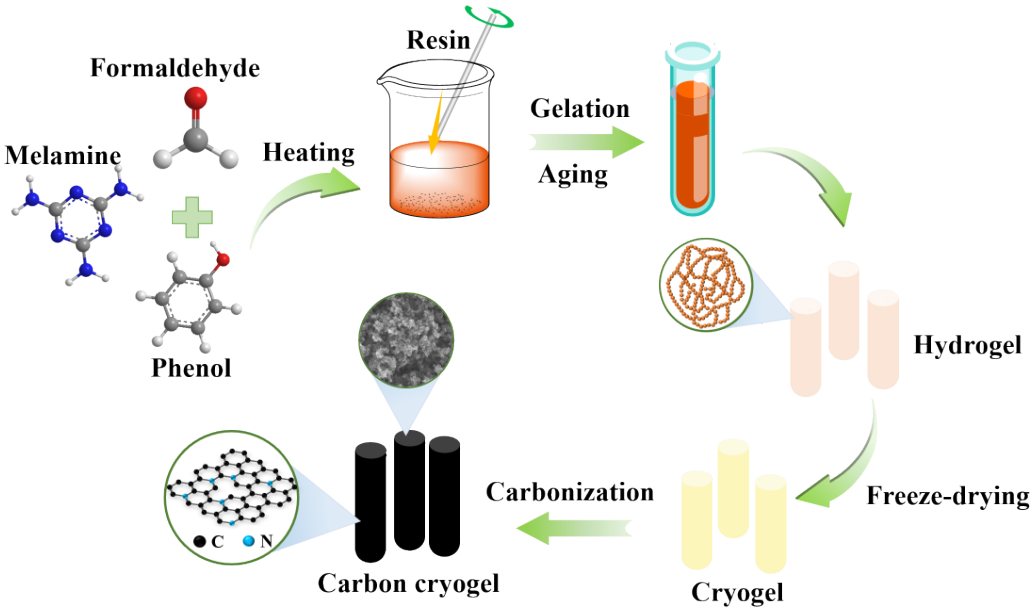

Fig. 1 Preparation method of PMF cryogels

2.3 Chemical characterization

The N_2 adsorption-desorption isotherms were obtained through an ASAP 2020 system (Micromeritics Instrument Corp., Norcross, USA) at 77 K. Before the adsorption experiment, the samples were degassed under 523 K vacuum for at least 24 h. The N_2 adsorption data were processed to determine the textural parameters [7, 8]. X-ray photoelectron spectroscopy (XPS) was performed on an ESCA PLUSOMICROM system equipped with a hemispherical electron energy analyzer. The spectrometer was operated under vacuum (< 5×10^{9} torr) with an analyzer of 50 eV for investigation scanning, 20 eV for detailed scanning, and carbon 1s peak of 284.5 eV for binding energy correction. The microstructure of carbon cryogels was examined by scanning electron microscopy (SEM; Semhitachis 3400, Hitachi, Japan). The X-ray diffraction (XRD) patterns of carbon cryogels were obtained by a Brook D8 advanced diffractometer with copper Kα radiation. Raman spectroscopy (DXR,

Thermo Fischer, Germany) was used for crystallographic characterization of the samples in the range of 500-2500 cm^{-1}.

The adsorption curves of CO_2 and N_2 at 0 and 25 ℃ under a pressure of 0-1 bar were obtained by the ASAP 2020 automatic instrument (Micromeritics Instrument Corp., Norcross, USA). The carbon cryogels was degassed at 473 K for at least 12 h prior to the measurement. The CO_2 adsorption isotherms were measured at 0 and 25 °C. These adsorption isotherms conformed to the Langmuir-Freundlich model [8]:

$$q = q_m \frac{K \times p^{\left(\frac{1}{c}\right)}}{1 + K \times p^{\left(\frac{1}{c}\right)}} \quad (1)$$

where q is the adsorption capacity at pressure p, mmol/g; q_m is the adsorption capacity at saturation, mmol/g; p is the partial pressure of CO_2, kPa; K and c are constants. According to the Langmuir Freundlich model, the pressure P corresponding to different values of adsorption capacity q was calculated. The ln(p) vs. 1/T curves were drawn, and the CO_2 adsorption isotherm was obtained using the slope of the curve. According to the Clausius-Clapeyron equation [8],

$$Q_{st} = -\Delta H \quad (2)$$

$$\ln(p) = -\frac{-\Delta H 1}{R\ T} + C \quad (3)$$

where Q_{st} is the equivalent adsorption heat, kJ/mol; ΔH is the adsorption enthalpy, kJ/mol; p is the CO_2 pressure, kPa; R is the gas constant, 8.314 J/(mol·K); T is the adsorption temperature, K. The CO_2/N_2 adsorption selectivity was calculated by the initial slope ratio as follows (Henry's law constant method): the first five data points on the single-component adsorption isotherm of CO_2/N_2 were selected, and the initial

slope of each isotherm was obtained by linear fitting. The adsorption selectivity was calculated as follows:

$$S = \frac{k_{CO_2}}{k_{N_2}} \quad (4)$$

3 Results and discussion

3.1 Textural and structural properties

Fig. 2a shows the XRD patterns of all the carbon cryogels, including the PF and the N-doped PMF carbon cryogels. All the samples show two major broad diffraction peaks near 22° and 43°, which are attributed to the (002) and (100/101) reflection planes, respectively. Further, no significant difference is found between PF and PMF carbon cryogels. All these carbon cryogels are amorphous carbon with turbostratic planes and randomly oriented graphitic layers [18, 35]. Fig. 2b shows the Raman spectrum of all the carbon cryogels, where two main peaks can be observed: the D band at 1340 cm^{-1} represents the defect of the C atomic lattice, and the G band at 1570 cm^{-1} represents the in-plane stretching vibration of C sp^2 hybridization [8, 33]. In general, the intensity ratio of D band to G band indicates the graphitization degree. The higher the value of I_D/I_G, the lower the molecular symmetry, i.e., the more defects in C atomic crystal. It can be seen that for the PMF carbon cryogels, with the increase in the molar ratio of F/(P+M), the value of I_D/I_G increases slightly from 0.939 to 0.974. This can be due to the difference in the extent of copolycondensation reaction during the hydrogel preparation process. In general, a lower ratio of I_D/I_G indicates that the graphitization degree is high, i.e., the content of formaldehyde does not affect the crystal structure greatly, which is consistent with the results of XRD analysis.

However, compared with the PMF cryogels, the pure PF carbon cryogel exhibits the lowest value of I_D/I_G (0.86). This can be attributed to the fact that the PMF cryogels have more defects due to the nitrogen doping [33].

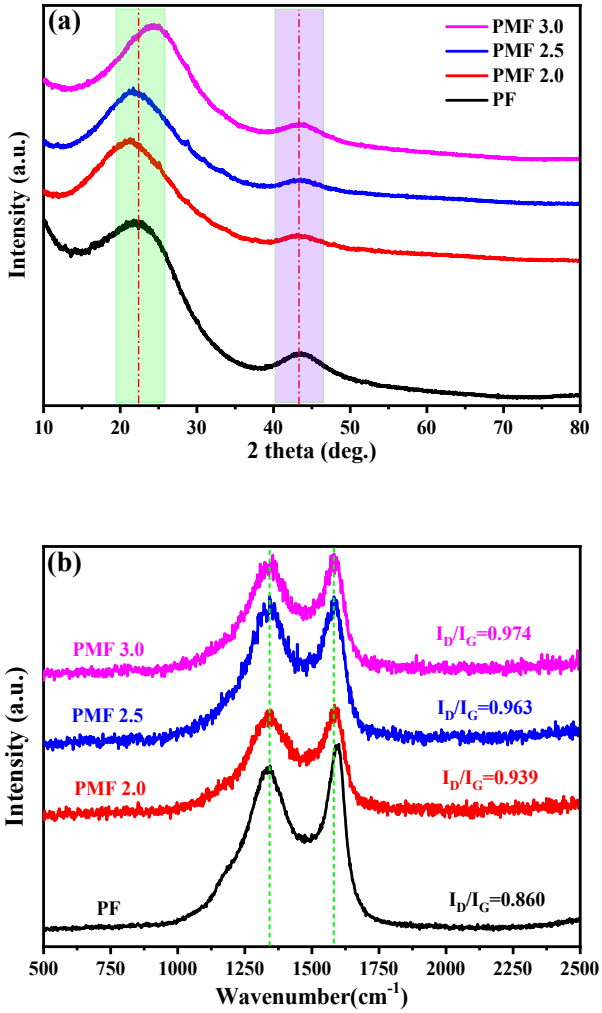

Fig. 2 (a) XRD patterns and (b) Raman spectra of all the carbon cryogels.

The N_2 adsorption-desorption isotherms of all the carbon cryogels are shown in Figure 3a. According to IUPAC classification, all the isotherms represent a combination of type I and IV isotherms, suggesting that micropores and mesopores exist simultaneously [8, 36]. At extremely low relative pressure, the adsorption amount increases sharply, indicating the presence of abundant micropores. The

hysteresis loops at higher pressure are related to the existence of mesoporous materials. The adsorption amount of PMF2.0 is much higher than that of the other samples, demonstrating that PMF2.0 has obviously higher specific surface area, pore volume, and especially micropores. On the contrary, the sample PF has the lowest N_2 adsorption capacity. It is interesting to note that all the samples show H3 type hysteresis loops at high relative pressure, indicating that these samples have both mesopores and macropores, which may be due to the formation of long and narrow pores by the accumulation of gel particles [8]. The isotherms of samples PMF2.5 and PMF3.0 almost coincide when the pressure P/P_0 is lower than 0.8, which may be because they have similar micropore volume. For higher pressure $P/P_0 > 0.8$, the increase in the adsorption of sample PMF3.0 is more significant, indicating that it has a larger amount of mesopores and macropores [37]. The above results are further confirmed by the pore size distribution (PSD) curves of carbon cryogels shown in Fig. 3b. It is clear that all the samples contain both mesopores and micropores, suggesting the existence of a hierarchical pore structure. For the PF carbon cryogels, the pores are mainly ultrafine pores with size less than 0.5 nm, which makes it difficult to realize CO_2 adsorption efficiently [35]. It is quite obvious that the sample PMF2.0 has more micropores (< 2 nm) with three peaks at 0.5, 0.8, and 1.2 nm, which is favorable for CO_2 adsorption [8].

The textural parameters are listed in Table 1. As expected, the PF carbon cryogel has the lowest specific surface area, total pore volume, micropore volume, and mesopore volume, which are 800.2 m^2/g, 0.46 cm^3/g, 0.32 cm^3/g, and 0.14 cm^3/g,

respectively. It mainly contains micropores, and the $V_{DR}/V_{0.99}$ is as high as 0.67. For the PMF carbon cryogels, as the molar ratio F/(P+M) increases, the specific surface area decreases from 1160.6 m^2/g to 874.1 m^2/g, the micropore volume linearly decreases from 0.47 cm^3/g to 0.35 cm^3/g, and the average pore width is reduced from 0.72 nm to 0.56 nm. All these results indicate that lower F/(P+M) molar ratio is conducive to the formation of more pores (micropores and mesopores), which is due to the relatively different extents of hydroxymethylation and polycondensation reaction and thus different degrees of cross-linking of the prepared carbon precursor. This has a significant impact on the subsequent drying and carbonization processes, thereby affecting the pore structure of carbon cryogels [18], which is consistent with previous reports that suggested that the synthesis conditions affect the textural properties of porous polymers [27, 37]. We speculate that a high F/(P+M) molar ratio leads to faster and higher cross-linking, causing rapid precipitation of polymers. Therefore, the synthesized PMF cryogel is dense and exhibits more shrinkage during the drying and carbonization processes. Finally, the nano polymer particles formed are more condensed, leading to lower surface area.

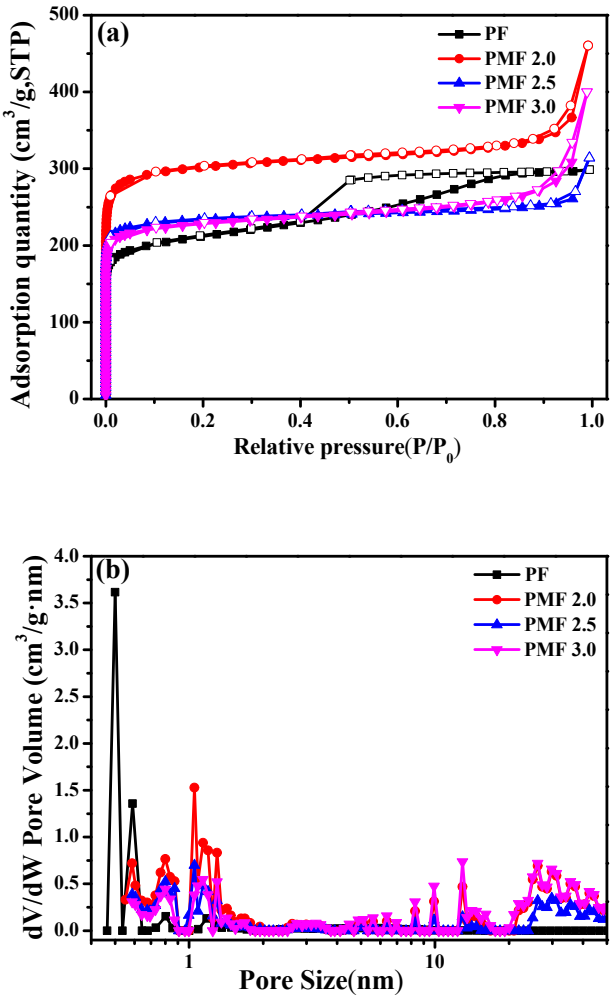

Fig.3 (a) N_2 adsorption-desorption curves of all the carbon cryogels; (b) pore size distribution of the carbon cryogels obtained by non-localized density functional theory (NLDFT).

Table 1. Pore structure parameter of carbon cryogels

Sample	S_{BET} (m^2/g)	$V_{0.99}$ (cm^3/g)	V_{DR} (cm^3/g)	L_0 (nm)	$V_{DR}/V_{0.99}$	V_{meso} (cm^3/g)	$V_{0.6}$ (cm^3/g)	$V_{0.6-0.8}$ (cm^3/g)	$V_{0.8-1.0}$ (cm^3/g)	$V_{1.0-1.5}$ (cm^3/g)
PMF 2.0	1160.6	0.71	0.47	0.72	0.66	0.24	0.236	0.047	0.040	0.056
PMF 2.5	904.6	0.49	0.36	0.56	0.75	0.12	0.221	0.034	0.025	0.026
PMF 3.0	874.1	0.62	0.35	0.57	0.57	0.26	0.228	0.020	0.011	0.026
PF	800.2	0.46	0.32	0.62	0.69	0.14	0.202	0.011	0.002	0.026

Fig. 4a-d shows the SEM images of all the carbon cryogels. It can be seen that

the carbon cryogels have a three-dimensional network structure formed by the agglomeration of spherical particles. The spherical particles aggregate to form small clusters, and obvious mesopores and macropores can be seen between the clusters. The SEM images of the three PMF carbon cryogels are slightly different. The sample PMF2.0 exhibits the smallest cluster size. As the molar ratio F/(P+M) increases, the microstructure become denser and the porosity decreases. This variation is more pronounced for the PF carbon cryogel, which is one of the densest samples. The condensed nano polymer particles lead to lower surface areas, which is consistent with the results of N_2 adsorption-desorption analysis [27, 37]. Figure 4e and 4f show the appearance and compression of organic and carbon PMF2.0 cryogels. It can be seen that both organic and carbon cryogels maintain good monolithic structure and have extremely low density and excellent mechanical strength, which can resist the compression of blocks that are hundred times its own mass.

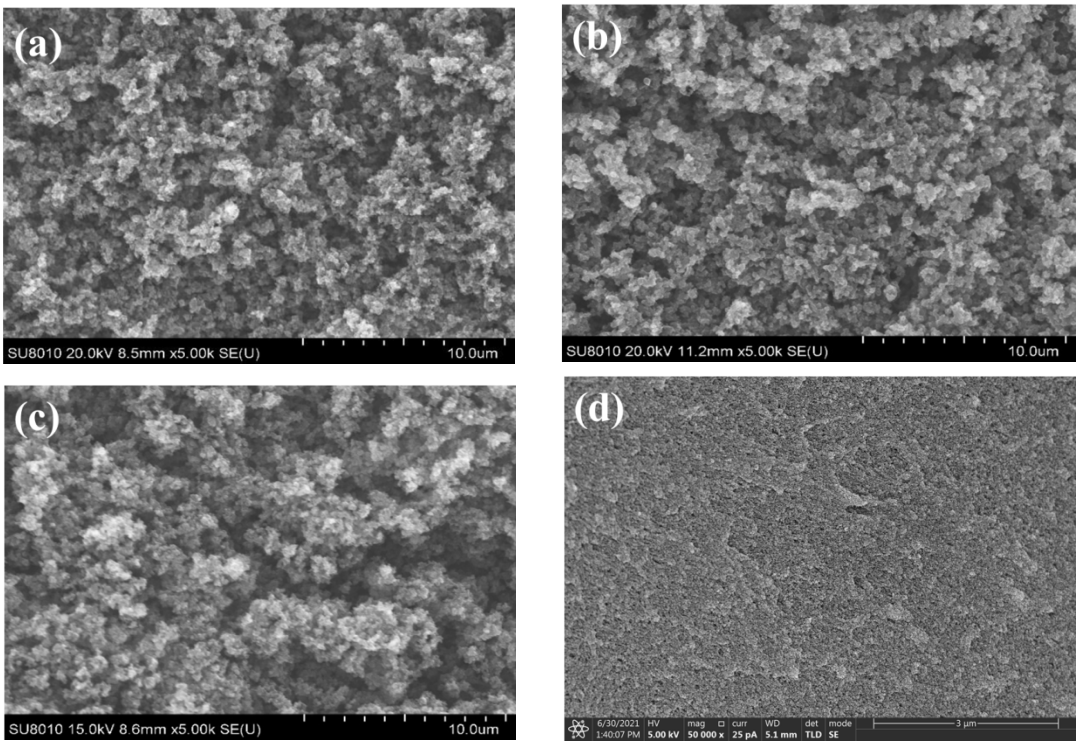

Fig. 4 SEM images of all the carbon cryogels: (a) PMF 2.0 at 5000x magnification, (b) PMF 2.5 at 5000x magnification, (c) PMF 3.0 at 5000x magnification, (d) PF at 50000x magnification; (e) PMF2.0 organic cryogel under compression; (f) PMF2.0 carbon cryogel under compression.

3.2 Surface characterization

Fig. 3a and 3b show the XPS spectrum of organic and carbon cryogels, respectively. It is clear that both organic and carbon cryogels show three peaks at 285, 400, and 532 eV, which can be ascribed to C 1s, N 1s, and O 1s respectively. The elemental content of the cryogels is given in Table 2. The C and O contents of organic PF cryogel are 83.72 % and 16.28%, respectively. With the addition of melamine, the C content decreases to the range of 74.17-77.63%, while the O content decreases to the range of 13.92-14.22%. The N content decreases to 8.45-11.62% with the increase in the molar ratio F/(P+M). The variation in the N content with molar ratio F/(P+M) can be due to the inhomogeneous polymerization of phenol and melamine [38]. It must be noted that all these organic PMF cryogels are promising precursors for preparing N-doped carbon materials due to the high N content. Compared with organic cryogels, the C element content in carbon cryogel is higher, while the N and O element contents are significantly lower. The C and O contents of PF carbon cryogel are 94.04 % and 5.96%, respectively. The contents of the C, O, and N

elements in the PMF carbon cryogels are in the range of 89.17-91.80%, 6.56-9.15%, and 1.57-1.68%, respectively. These results confirm the successful preparation of N-doped cryogels. However, the three PMF carbon cryogels have nearly the same N content, which is not very high (less than 2%). This may be because the majority of N species localized on or near the surface of PMF cryogels burn off during the carbonization process [8, 33].

Furthermore, the C1s XPS spectrum of carbon cryogels can be decomposed into five components [15, 39-42]: graphitic carbon (sp^2 configuration, 284.6 eV), Csp^2-N/C-OH (285.6 eV), Csp^3-N/C=O (287.1 eV), carboxyl (289.2 eV), and aromatic ring π-π* transition (291.2 eV) (Fig. 3c-e). According to Table 3, there is basically no difference in the proportion of each carbon element in the sample. Compared with the other two samples, the Csp^3-N/C=O (287.1 eV) and π-π* transitions of sample PMF2.0 increase slightly. The N1s spectrum can be decomposed into four components [8, 15, 38, 42-44]: pyridinic-N (N-6，398.1 eV), pyridonic-N (N-5，399.1 eV), quaternary-N (N-Q，400.8 ± 0.1 eV), and pyridine N-oxide (N-X，402.7 ± 0.1 eV) (Fig. 3f-h). The nitrogen atoms in the graphene layers of PMF carbon cryogels are preferentially located at the positions with lower energy, such as N-6, N-5, and N-Q [38]. As shown in Table 3, the proportion of N-Q is the highest, and with the increase in the formaldehyde content, its value increases. However, N-5 and N-X show the opposite trend, i.e., with the increase in the amount of formaldehyde, the proportion of N-Q decreases. This suggests that an increase in the amount of formaldehyde may cause the conversion of N-5 and N-X to N-Q. O1s spectrum can

be decomposed into four components [15, 43]: C=O in ketone/carbonyl (530.9 eV), O-C in lactone, phenol/ether/epoxy (532.5 eV), C=O in carboxylic acid (534.0 eV), and occluded CO or CO_2 (536 eV) (Fig. 3i-k). As shown in Table 3, the O1s spectrum mainly includes O-C in lactone and C=O in carboxylic acid. O-C in lactone is related to the methylene ether bonds formed during the formation of cryogel. With the increase in the formaldehyde content, the proportion of O-C in lactone decreases, which may be due to the increase in the cross-linking density, forming more stable bonds.

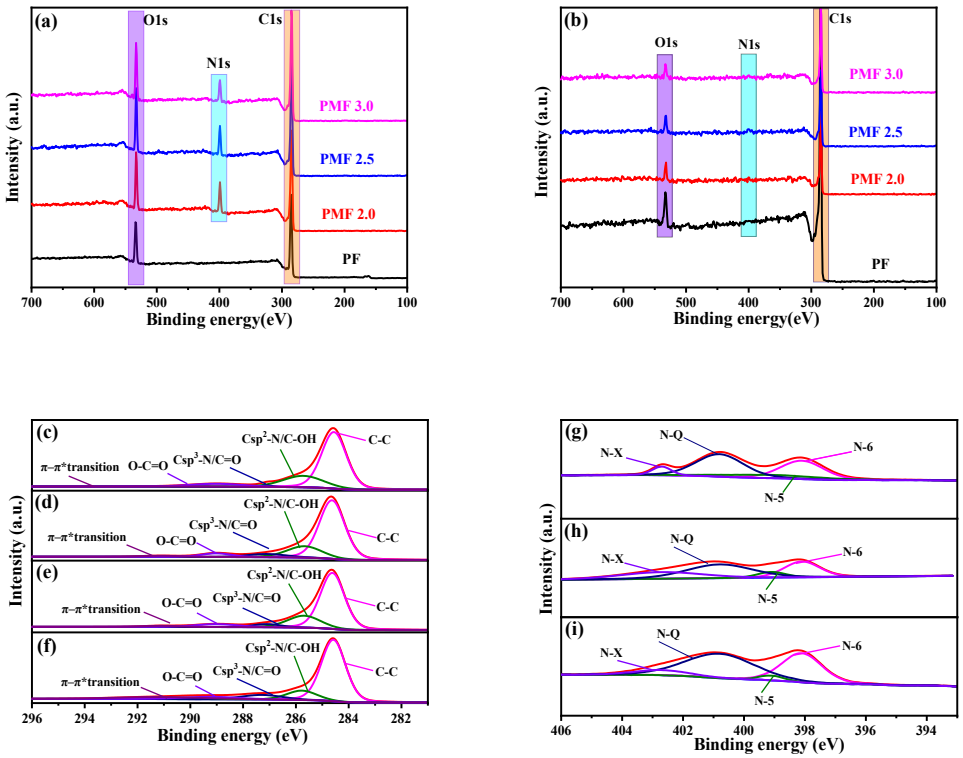

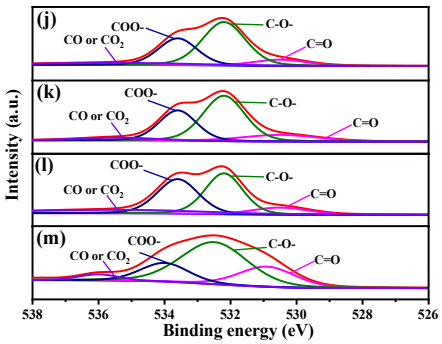

Fig.4 XPS survey spectrum of organic (a) and carbon cryogels (b); C1s core level spectra of carbon cryogel: (c) PMF 2.0, (d) PMF 2.5, (e) PMF 3.0, and (f) PF; N1s core level spectra of carbon cryogel: (g) PMF 2.0, (h) PMF 2.5, and (i) PMF 3.0; O1s core level spectra of carbon cryogel: (j) PMF 2.0, (k) PMF 2.5, (l) PMF 3.0, and (m) PF.

Table 2. Relative elemental content of organic and carbon cryogels

Sample	Relative elemental content %		
	C	N	O
Organic PMF 2.0	74.17	11.62	14.22
Organic PMF 2.5	76.24	9.80	13.96
Organic PMF 3.0	77.63	8.45	13.92
Organic PF	83.72	/	16.28
Carbon PMF 2.0	90.32	1.57	8.11
Carbon PMF 2.5	89.17	1.68	9.15
Carbon PMF 3.0	91.80	1.64	6.56
Carbon PF	94.04	/	5.96

Table 3. Ratio of various C-, N-, and O-containing bonds (%)

	C element					N element				O element			
	C-C	Csp^2-N/C-OH	Csp^3-N/C=O	O-C=O	π-π*transition	N-6	N-5	N-Q	N-X	C=O	C-O-	COO-	Occluded CO or CO_2
	284.6±0.1eV	285.6±0.2eV	287.1eV	289.0±0.2eV	290.0±0.1eV	398.3±0.3eV	399.1±0.2eV	400.8±0.1eV	402.7±0.5eV	530.7±0.2eV	532.2±0.1eV	533.6±0.2eV	535.6±0.2eV
PMF 2.0	68.2	20.4	4.5	5.5	1.4	26.5	12.1	34.1	27.3	8.9	56.4	30.3	4.5
PMF 2.5	65.8	22.8	3.9	5.8	1.6	33.0	10.4	37.4	19.1	13.6	51.0	30.0	5.4
PMF 3.0	64.2	20.6	6.5	5.6	3.2	26.7	9.5	45.8	18.1	11.1	43.5	36.8	8.6
PF	65.0	12.3	8.4	6.2	8.1	/	/	/	/	22.4	54.9	17.8	4.9

3.3 CO_2 adsorption property

Fig. 5a shows the CO_2 adsorption isotherms of the four carbon cryogel samples at 273 K. All the isotherms exhibit the same trend, i.e., the adsorption capacity increases with the increase in pressure. As shown in Table 4, the CO_2 uptakes for PF, PMF2.0, PMF2.5, and PMF3.0 carbon cryogels are 3.98, 5.79, 4.85, and 4.99 mmol/g, respectively. It is clear that PF and PMF2.0 have the lowest and highest CO_2 adsorption capacities, respectively, indicating that PMF2.0 carbon cryogel is more conducive to the adsorption of CO_2. Furthermore, with the increase in the molar ratio of F/(P+M), the CO_2 adsorption capacities of PMF carbon cryogels decreases from 5.79 mmol/g to 4.85 mmol/g. The CO_2 adsorption isotherms show the same tendency, and the adsorption capacities are listed in Table 4.

There are two main reasons for the differences in the CO_2 adsorption capacities among the samples. Firstly, the surface area and the pore volume, especially the micropore volume and the ultra-micropore volume, is the main factor controlling the physisorption of CO_2 onto the porous carbon materials [3]. According to previous reports, smaller micropores are more conducive to the adsorption of CO_2, especially the ultra-micropores smaller than 0.8 nm have the best adsorption effect on CO_2 [2, 35, 45]. As can be seen in Figure 2b, the pore size of PMF2.0 carbon cryogels (less than 1 nm) is obviously higher than that of PMF2.5 and PMF3.0 carbon cryogels, so their CO_2 adsorption capacity is also higher than that of the other two samples. In addition, although the micropore volume of PF carbon cryogel sample is not very low (0.32 cm^3/g), its CO_2 adsorption capacity is extremely low. This is because the

molecular diameter of CO_2 is 0.33 nm, which is generally adsorbed in a single layer, and then the two sides of the pore are two layers, i.e., the pore size of nearly 0.7 corresponds to the maximum adsorption efficiency. The pores of PF carbon cryogel mainly include ultrafine pores with size less than 0.5 nm, which makes it difficult to realize CO_2 adsorption efficiently [25]. Figure 5b shows the relationship between surface area (S_{BET}), micropore volume (V_{DR}), and CO_2 adsorption capacity. The CO_2 adsorption capacity increases with both S_{BET} and V_{DR} due to the more adsorption sites. By further refining the pore size and examining its relationship with CO_2 adsorption performance, it can be found that the pore size less than 0.8 nm is more beneficial for CO_2 adsorption. The correlation coefficient between the micropore volume with pore size less than 0.8 nm and the CO_2 adsorption capacity at 0 °C can reach 0.96.

Secondly, the effect of N heteroatom introduced in PMF carbon cryogels is reflected in the CO_2 – N species interaction within the cryogels [3]. The N doping can improve the electron donor properties of carbon by affecting its spin density, leading to an increase in the isosteric heat of adsorption and chemisorption of adsorbents [35]. The calculated isosteric adsorption heat (Qst) of both PF and PMF2.0 carbon cryogels is shown in Figure 5c. The adsorption heat of samples PF and PMF2.0 under low adsorption capacity is 30.85 and 33.06 kJ/mol, respectively. These values are all much higher than the Qst of porous carbon materials (17 kJ/mol). PMF carbon cryogel has a higher Qst than PF carbon cryogel, which indicates that apart from physical adsorption, chemical adsorption can also occur during the initial stage of CO_2

adsorption. Therefore, the high heat of adsorption of the sample is due to the presence of a large number of micropores and the interaction between the nitrogen-containing groups with CO_2.

The selective adsorption of CO_2 over N_2 is another important criterion used to evaluate the adsorption performance of CO_2, and the corresponding values are shown in Fig. 5d. The selective adsorption of CO_2/N_2 can be obtained by calculating the slope ratio, as shown in Table 5. It can be found that the selectivity of PMF carbon cryogels are in the range of 12.53-14.55, which is higher than that of PF carbon cryogel (11.79). This can be ascribed to the synergistic effect of N doping and suitable pore structure. The PMF2.0 carbon cryogel, which has the highest CO_2 adsorption capacity, also has quite high selective adsorption value of CO_2/N_2 (13.43). Compared with other carbon materials, the selectivity of PMF carbon cryogels are comparable or even superior, and thus they can be used as an ideal separation material for gas mixtures. This can be explained by two facts. Firstly, CO_2 has higher polarizability and quadrupole moment than N_2, which leads to a strong adsorption and causes a high adsorption amount through micropores in the low pressure range [46]. Secondly, the existence of heteroatoms N and O can increase the polarity of the carbon cryogels, thereby enhancing the selectivity, which is similar to the selectivity trend of other N-doped carbon materials.

Table 4. CO_2 adsorption and selective adsorption of CO_2 over N_2 of carbon cryogels

	PMF 2.0	**PMF 2.5**	**PMF 3.0**	**PF**
CO_2 adsorption (0 °C/25 °C, mmol/g at 1 bar)	5.79/3.68	4.85/3.23	4.99/3.62	3.98/2.78

Selective adsorption of CO_2/N_2	13.43	12.53	14.55	11.79

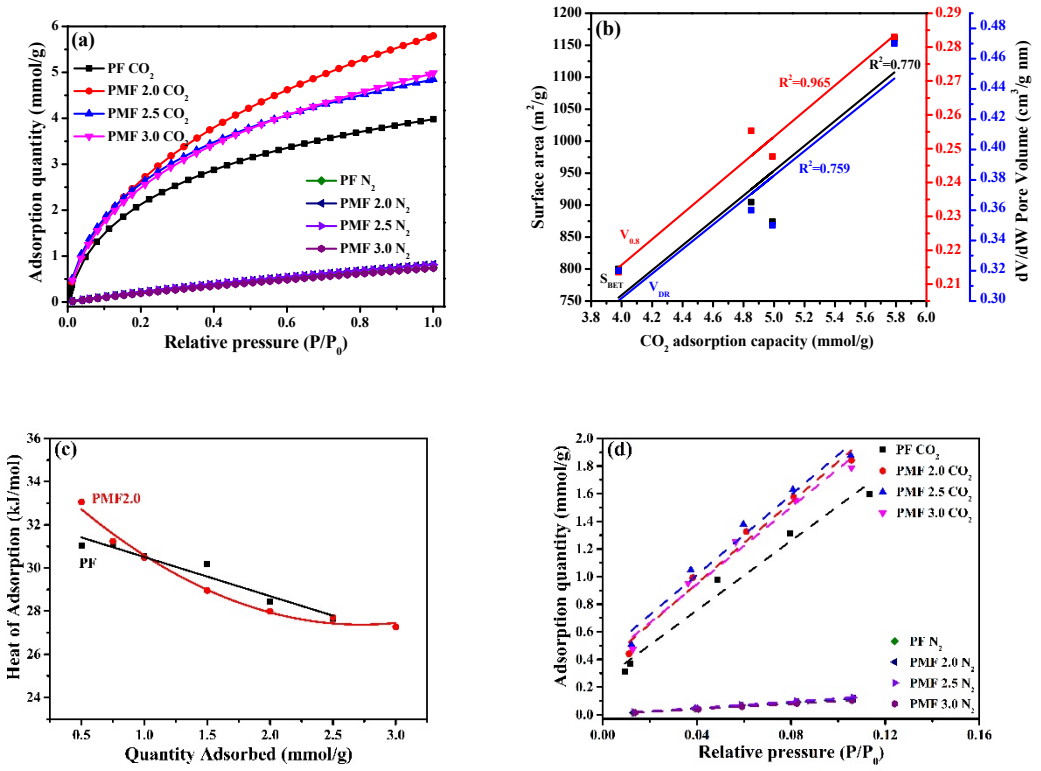

Fig. 5 (a) CO_2 adsorption isotherms of carbon cryogels at 0 °C; (b) correlation between textural parameters and CO_2 adsorption capacity; (c) Qst of carbon cryogels at various adsorption quantities; (d) initial slope from CO_2 and N_2 adsorption in the pressure range of less than 0.11 bar for CO_2/N_2 selectivity calculation.

Table 5 compares the properties of carbon gels prepared by different raw materials and drying methods. It is observed that the prepared carbon cryogels in this study have relatively higher specific surface area. Their CO_2 adsorption capacity is also higher than that of most of the carbon aerogels [2, 47, 48], cryogels [7, 49], and xerogels [19, 50, 51] reported earlier. In addition, the performance of the prepared carbon cryogels is comparable to that of some previously reported nitrogen-doped porous carbon materials [52-54]. Their carbon dioxide adsorption performance is also comparable or even much better than that of these materials. These results indicate

that the prepared PMF carbon cryogels with N doping and suitable PSD is a promising adsorbent for CO_2 capture.

Table 5. Comparison of the material characteristics and CO_2 adsorption capacities of carbon gels and N doped carbon materials

Samples	N content (%)	S_{BET} (m^2/g)	V_{DR} (cm^3/g)	CO_2 uptake (mmol/g)	Ref
Cryogel PMF	1.57	1161	0.47	5.79 at 273 K 3.68 at 298 K	This paper
Cryogel PUF	2.08	1710	0.64	5.51 at 273 K	[7]
Cryogel CP	-	679	0.32	5.72 at 298 K	[49]
Xerogel RUF	0.51	577	0.18	4.50 at 273 K	[19]
Xerogel MF	-	1090	-	2.20 at 298 K	[50]
Xerogel RF	-	888	0.26	2.80 at 298 K	[51]
Aerogel RF	-	1521	0.99	3.00 at 298 K	[2]
Aerogel RF	-	1083	1.92	1.91 at 298 K	[47]
Aerogel RF	-	900	-	1.33 at 308 K	[48]
Porous carbon NPC800	2.73	2958	1.16	6.24 at 273 K 3.36 at 298 K	[52]
Porous carbon SG-CN(2)	3.40	1111	0.33	3.34 at 298 K	[53]
Porous carbon P80	8.05	891	0.32	4.40 at 273 K 2.98 at 298 K	[54]
Porous graphene aerogels	22.97	167.66	-	1.18 at 298 K	[55]
Porous carbon N-HPC	4.7	1960	-	3.3 at 273 K 2.0 at 298 K	[56]
Porous carbon PCMSs-900	1.25	642	0.27	4.3 at 273 K 3.0 at 298 K	[57]

4 Conclusions

PMF carbon cryogels with excellent properties were synthesized by using sol-gel

and freeze-drying process with low-cost formaldehyde, phenol, and melamine as raw materials. The effect of molar ratio of F/(P+M) on the pore structure, chemical properties, and CO_2 adsorption performance was examined. For comparison, the PF carbon cryogel without N doping was prepared, which showed the lowest surface area, pore volume, and CO_2 adsorption capacity. The PMF carbon cryogels could retain their monolithic structure after drying and carbonization processes, indicating their good mechanical property. With the increase in the molar ratio of F/(P+M), the specific surface area, total pore volume, and micropore volume decreased. The carbon cryogel PMF2.0 exhibited the highest specific surface area and micropore volume, which were 1160.6 m^2/g and 0.47 cm^3/g, respectively, thus it showed the maximum CO_2 adsorption capacities of 5.79 and 3.85 mmol/g at 273 and 298 K, respectively, under 1 bar. The micropores, especially those with size less than 0.8 nm, were more conducive to the absorption of CO_2. In addition, the PMF2.0 carbon cryogel sample exhibited high CO_2/N_2 adsorption selectivity (13.43) and high isosteric adsorption heat (33.06 kJ/mol). This excellent CO_2 adsorption performance was mainly attributed to the synergistic effect of heteroatom N doping and abundant pores with suitable distribution, indicating the excellent potential of carbon cryogel in CO_2 capture.

Acknowledgements

The authors are grateful for the financial support from the National Natural Science Foundation of China (31971593), the Natural Science Foundation of Fujian Province Department of Science and Technology (2019J01386), National Natural Science Foundation of China

(32071688).

Reference

[1] D.H. Jeon, B.G. Min, J.G. Oh, C. Nah, S.J. Park, Influence of nitrogen moieties on CO_2 capture of carbon aerogel, Carbon lett, 16 (2015) 57-61.

[2] C. Robertson, R. Mokaya, Microporous activated carbon aerogels via a simple subcritical drying route for CO_2 capture and hydrogen storage, Micropor. Mesopor. Mat, 179 (2013) 151-156.

[3] G. Singh, K.S. Lakhi, S. Sil, S.V. Bhosale, I.Y. Kim, K. Albahily, A. Vinu, Biomass derived porous carbon for CO_2 capture, Carbon 148 (2019) 164-186.

[4] K. Kamal, D.I. Grekov, A.M. Shariff, M.A. Bustam, P. Pré, Improving textural properties of magnesium-based metal-organic framework for gas adsorption by carbon doping, Micropor. Mesopor. Mat, (2021) 111246.

[5] L. Luo, T. Chen, Z. Li, Z. Zhang, W. Zhao, M. Fan, Heteroatom self-doped activated biocarbons from fir bark and their excellent performance for carbon dioxide adsorption, J. CO_2 Util, 25 (2018) 89-98.

[6] J. Srenscek-Nazzal, K. Kielbasa, Advances in modification of commercial activated carbon for enhancement of CO_2 capture, Appl. Surf. Sci, 494 (2019) 137-151.

[7] Z. Li, T. Chen, X. Wu, L. Luo, Z. Zhang, Z. Li, M. Fan, Z. Su, W. Zhao, Nitrogen-containing high surface area carbon cryogel from co-condensed phenol–urea–formaldehyde resin for CO_2 capture, J. Porous Mat, 26 (2018) 847-854.

[8] Z.L. Li, Y.L. Zhou, W. Yan, L. Luo, Z.Z. Su, M.Z. Fan, S.R. Wang, W.G. Zhao, Cost-effective monolithic hierarchical carbon cryogels with nitrogen doping and high-performance mechanical properties for CO_2 capture, ACS Appl. Mater. Interfaces 12 (2020) 21748-21760.

[9] F. Othman, N. Yusof, S. Samitsu, N. Abdullah, N. Wan, Activated carbon nanofibers incorporated metal oxides for CO_2 adsorption: Effects of different type of metal oxides, J. CO_2 Util, 45 (2021) 101434.

[10] A. Lai, H.C. Loehde-Woolard, W.W. Mcneary, J. Burger, A.W. Weimer, Amine-functionalized fumed silica for CO_2 capture through particle molecular layer deposition, Chem. Eng. Sci, 245 (2021) 116954.

[11] E. Luzzi, P. Aprea, M. Luna, D. Caputo, G. Filippone, Mechanically coherent zeolite 13X/chitosan aerogel beads for effective CO_2 capture, ACS Appl. Mater. Interfaces, 13 (2021) 20728-20734.

[12] Y. Yang, Y.C. Chong, T.H. Bae, Polyamine-appended porous organic copolymers with controlled structural properties for enhanced CO_2 capture, ACS Sustain. Chem. Eng, 9 (2021) 2017-2026.

[13] J. Wang, Q. Pu, P. Ning, S. Lu, Activated carbon-based composites for capturing CO_2: A review, Greenh. Gases 11 (2021) 377-393.

[14] F. Guo, Y. Jiang, Z. Xu, Y. Xiao, B. Fang, Y. Liu, W. Gao, P. Zhao, H. Wang, C. Gao, Highly stretchable carbon aerogels, Nat. Commun, 9 (2018) 881.

[15] G. Rasines, P. Lavela, C. Macías, M.C. Zafra, J.L. Tirado, J.B. Parra, C.O. Ania, N-doped monolithic carbon aerogel electrodes with optimized features for the electrosorption of ions, Carbon 83 (2015) 262-274.

[16] C. Moreno-Castilla, F.J. Maldonado-Hódar, Carbon aerogels for catalysis applications: An overview, Carbon 43 (2005) 455-465.

[17] B. Khalid, Q. Meng, J. Li, B. Cao, Nitrogen rich graphene-cross-linked melamine formaldehyde carbon cryogels for supercapacitors, Electrochim. Acta, 142 (2014) 101-107.

[18] S. Mezzavilla, C. Zanella, P.R. Aravind, C. Della Volpe, G.D. Sorarù, Carbon xerogels as electrodes for supercapacitors. The influence of the catalyst concentration on the microstructure and on the electrochemical properties, J. Mater. Sci, 47 (2012) 7175-7180.

[19] A.S. Ello, J.A. Yapo, A. Trokourey, N-doped carbon aerogels for carbon dioxide (CO_2) capture, Afr. J. Pure Appl. Chem. 7 (2013) 61-66.

[20] S.E. Muehlemann, L. Huber, S. Zhao, S.K. Matam, M.M. Koebel, Facile synthesis of resorcinol-melamine-formaldehyde based carbon xerogel, Mater. Today: Proceedings 5 (2018) 13776–13784.

[21] L. Wang, J. Wang, L. Zheng, Z. Li, L. Wu, X. Wang, Superelastic, anticorrosive, and flame-resistant nitrogen-containing resorcinol formaldehyde/graphene oxide composite aerogels, ACS Sustain. Chem. Eng, 7 (2019) 10873-10879.

[22] B. Nagy, I. Bakos, I. Bertóti, A. Domán, A. Menyhárd, M. Mohai, K. László, Synergism of nitrogen and reduced graphene in the electrocatalytic behavior of resorcinol-formaldehyde based

carbon aerogels, Carbon 139 (2018) 872-879.

[23] N. Job, F. Panariello, J. Marien, M. Crine, J.-P. Pirard, A. Léonard, Synthesis optimization of organic xerogels produced from convective air-drying of resorcinol–formaldehyde gels, J. Non-Cryst. Solids 352 (2006) 24-34.

[24] N. Job, R. Pirard, J. Marien, J.P. Pirard, Porous carbon xerogels with texture tailored by pH control during sol–gel process, Carbon 42 (2004) 619-628.

[25] A.C. Pierre, G.r.M. Pajonk, Chemistry of aerogels and their applications, Chem. Rev, 102 (2002) 4243-4265.

[26] D. Long, X. Liu, W. Qiao, R. Zhang, L. Zhan, L. Ling, Molecular design of polymer precursors for controlling microstructure of organic and carbon aerogels, J. Non-Cryst. Solids 355 (2009) 1252-1258.

[27] D. Wu, R. Fu, Z. Yu, Organic and carbon aerogels from the NaOH-catalyzed polycondensation of resorcinol-furfural and supercritical drying in ethanol, J. Appl. Polym. Sci, 96 (2005) 1429-1435.

[28] S. Araby, A. Qiu, R. Wang, Z. Zhao, C.H. Wang, J. Ma, Aerogels based on carbon nanomaterials, J. Mater. Sci. 51 (2016) 9157-9189.

[29] Y. Zhu, H. Hu, W. Li, H. Zhao, Preparation of cresol–formaldehyde carbon aerogels via drying aquagel at ambient pressure, J. Non-Cryst. Solids 352 (2006) 3358-3362.

[30] X. Yang, D. Yang, G. Zhang, H. Zuo, Preparation of mesoporous carbon aerogels via ambient pressure drying using a self-sacrificing melamine-formaldehyde template, J. Power Sources 482 (2021) 229135.

[31] N. Job, A. Théry, R. Pirard, J. Marien, L. Kocon, J.N. Rouzaud, F. Béguin, J.P. Pirard, Carbon aerogels, cryogels and xerogels: Influence of the drying method on the textural properties of porous carbon materials, Carbon 43 (2005) 2481-2494.

[32] A. Szczurek, G. Amaral-Labat, V. Fierro, A. Pizzi, A. Celzard, The use of tannin to prepare carbon gels. Part II. Carbon cryogels, Carbon 49 (2011) 2785-2794.

[33] A. Kalijadis, N. Gavrilov, B. Jokić, M. Gilić, A. Krstić, I. Pašti, B. Babić, Composition, structure and potential energy application of nitrogen doped carbon cryogels, Mater. Chem. Phys, 239 (2020) 122120.

[34] K.Y. Kang, B.I. Lee, J.S. Lee, Hydrogen adsorption on nitrogen-doped carbon xerogels, Carbon

47 (2009) 1171-1180.

[35] S. Balou, S.E. Babak, A. Priye, Synergistic effect of nitrogen doping and ultra-microporosity on the performance of biomass and microalgae-derived activated carbons for CO_2 capture, ACS Appl. Mater. Interfaces 12 (2020) 42711-42722.

[36] D. Mallesh, J. Anbarasan, P.M. Kumar, K. Upendar, N. Lingaiah, Synthesis, characterization of carbon adsorbents derived from waste biomass and its application to CO_2 capture, Appl. Surf. Sci, 530 (2020) 147226.

[37] H. Cui, H. Chen, Z. Guo, J. Xu, J. Shen, Preparation of high surface area mesoporous melamine formaldehyde resins, Micropor. Mesopor. Mat, (2020) 110591.

[38] D. Long, J. Zhang, J. Yang, Z. Hu, G. Cheng, X. Liu, R. Zhang, L. Zhan, W. Qiao, L. Ling, Chemical state of nitrogen in carbon aerogels issued from phenol–melamine–formaldehyde gels, Carbon 46 (2008) 1259-1262.

[39] K. Li, M. Zhou, L. Liang, L. Jiang, W. Wang, Ultrahigh-surface-area activated carbon aerogels derived from glucose for high-performance organic pollutants adsorption, J. Colloid Interface Sci, 546 (2019) 333-343.

[40] H. Zhang, J. Feng, L. Li, Y. Jiang, J. Feng, Controlling the microstructure of resorcinol–furfural aerogels and derived carbon aerogels via the salt templating approach, RSC Adv. 9 (2019) 5967-5977.

[41] J. Yu, M. Guo, F. Muhammad, A. Wang, G. Yu, H. Ma, G. Zhu, Simple fabrication of an ordered nitrogen-doped mesoporous carbon with resorcinol–melamine–formaldehyde resin, Micropor. Mesopor. Mat, 190 (2014) 117-127.

[42] S.M. Li, S.Y. Yang, Y.S. Wang, C.H. Lien, H.W. Tien, S.T. Hsiao, W.H. Liao, H.P. Tsai, C.L. Chang, C.C.M. Ma, C.C. Hu, Controllable synthesis of nitrogen-doped graphene and its effect on the simultaneous electrochemical determination of ascorbic acid, dopamine, and uric acid, Carbon 59 (2013) 418-429.

[43] M. Seredych, D. Hulicova-Jurcakova, G.Q. Lu, T.J. Bandosz, Surface functional groups of carbons and the effects of their chemical character, density and accessibility to ions on electrochemical performance, Carbon 46 (2008) 1475-1488.

[44] G. Yang, H. Han, T. Li, C. Du, Synthesis of nitrogen-doped porous graphitic carbons using nano-

$CaCO_3$ as template, graphitization catalyst, and activating agent, Carbon 50 (2012) 3753-3765.

[45] M. Sevilla, A.B. Fuertes, Sustainable porous carbons with a superior performance for CO_2 capture, Energy Environ. Sci, 4 (2011) 1765.

[46] G. Sethia, A. Sayari, Comprehensive study of ultra-microporous nitrogen-doped activated carbon for CO_2 capture, Carbon 93 (2015) 68-80.

[47] M.L. M, C. P, C. M, Carbon aerogels used in carbon dioxide capture, Bol. Grupo Español Carbón (2016) 9-12.

[48] M. Anas, A.G. Gönel, S.E. Bozbag, C. Erkey, Thermodynamics of Adsorption of Carbon Dioxide on Various Aerogels, J. CO_2 Util, 21 (2017) 82-88.

[49] A.A. Alhwaige, H. Ishida, S. Qutubuddin, Carbon aerogels with excellent CO_2 adsorption capacity synthesized from clay-reinforced biobased chitosan-polybenzoxazine Nanocomposites, ACS Sustain. Chem. Eng, 4 (2016) 1286-1295.

[50] E. Masika, R. Mokaya, High surface area metal salt templated carbon aerogels via a simple subcritical drying route: preparation and CO_2 uptake properties, RSC Adv, 3 (2013) 17677.

[51] Q. Liu, P. He, X. Qian, Z. Fei, Z. Zhang, X. Chen, J. Tang, M. Cui, X. Qiao, Carbon aerogels synthesizd with cetyltrimethyl ammonium bromide (CTAB) as a catalyst and its application for CO_2 capture, Z. anorg. allg. Chem. 644 (2018) 155-160.

[52] X. Ma, L. Li, Z. Zeng, R. Chen, C. Wang, K. Zhou, H. Li, Experimental and theoretical demonstration of the relative effects of O-doping and N-doping in porous carbons for CO_2 capture, Appl. Surf. Sci, 481 (2019) 1139-1147.

[53] S.O. Adio, S.A. Ganiyu, M. Usman, I. Abdulazeez, K. Alhooshani, Facile and efficient nitrogen modified porous carbon derived from sugarcane bagasse for CO_2 capture: Experimental and DFT investigation of nitrogen atoms on carbon frameworks, Chem. Eng. J, 382 (2019) 122964.

[54] H. Cui, J. Xu, J. Shi, N. Yan, Y. Liu, Facile fabrication of nitrogen doped carbon from filter paper for CO_2 adsorption, Energy 187 (2019) 115936.

[55] A. Ap, A. Acc, B. Ab, A. Eg, Effect of synthesis conditions on CO_2 capture of ethylenediamine-modified graphene aerogels, Appl. Surf. Sci, 487 (2019) 228-235.

[56] D. Zhao, S. Wang, J. Qin, Y. Zhao, L. Duan, J. Wang, W. Gao, R. Wang, C. Wang, M. Pal, Z.S. Wu, Ultrahigh surface area N-doped hierarchically porous carbon for enhanced CO_2 capture and

electrochemical energy storage, ChemSusChem 12 (2019) 1-10.

[57] Y. Wang, M. Wang, Z. Wang, S. Wang, J. Fu, Tunable-quaternary (N, S, O, P)-doped porous carbon microspheres with ultramicropores for CO_2 capture, Appl. Surf. Sci, 507 (2019) 145130.